Mapping the role of aromatic amino acids within a blue-light sensing LOV domain

ARTICLE

Mapping the role of aromatic amino acids within a blue-light sensing LOV domain

1 \Received 00th January 20xx,
Accepted 00th January 20xx

DOI: 10.1039/x0xx00000x

Yonghong Ding,[a,b] Ziyue Zhao,[a] Jörg Matysik,[a] Wolfgang Gärtner [a] and Aba Losi[c]*

Photosensing LOV (Light, Oxygen, Voltage) domains detect and respond to UVA/Blue (BL) light by forming a covalent adduct between the flavin chromophore and a nearby cysteine, via the decay of the flavin triplet excited state. LOV domains where the reactive cysteine has been mutated are valuable fluorescent tools for microscopy and as genetically encoded photosensitisers for reactive oxygen species. Besides being convenient tools for applications, LOV domains without the reactive cysteine (naturally occurring or engineered) can still be functionally photoactivated via formation of a neutral flavin radical. Tryptophans and tyrosines are held as the main partners as potential electron donors to the flavin excited states. In this work, we explore the relevance of aromatic amino acids in determining the photophysical features of the LOV protein *Mr*4511 from *Methylobacterium radiotolerans* by introducing point mutations into the C71S variant that does not form the covalent adduct. By using an array of spectroscopical techniques we measured the fluorescence quantum yields and lifetimes, the triplet yields and lifetimes, and the efficiency of singlet oxygen (SO) formation for eleven Mr4511 variants. Insertion of Trp residues at distances between 0.6 and 1.5 nm from the Flavin chromophore results in strong quenching of the flavin excited triplet state and, at the shorter distances even of the singlet excited state. The mutation F130W (ca. 0.6 nm) completely quenches the singlet excited state, preventing triplet formation: in this case, even if the cysteine is present, the photo-adduct is not formed. Tyrosines are also quenchers for the flavin excited states, although not as efficient as Trp residues, as demonstrated with their substitution with the inert phenylalanine. For one of these variants, C71S/Y116F, we found that the quantum yield of formation for singlet oxygen is 0.44 in aqueous aerobic solution, vs 0.17 for C71S. Based on our study with *Mr*4511 and on literature data for other LOV domains we suggest that Trp and Tyr residues too close to the flavin chromophore (at distances less than 0.9 nm) reduce the yield of photoproduct formation and that introduction of inert Phe residues in key positions can help developing efficient, LOV-based photosensitisers.

Introduction

The acronym LOV (Light, Oxygen, Voltage) identifies UVA/Blue Light (BL) sensing domains with a typical PAS (Per, Arnt, Sim), α/β fold.[1] The LOV core encompasses ca. 110 aa, organized in the secondary structure elements named Aβ-Bβ-Cα-Dα-Eα-Fα-Gβ-Hβ- Iβ and with a highly conserved three-dimensional structure; these photosensitive domains bind a riboflavin derivative as chromophore in a 1:1 stoichiometry, preferentially FMN (flavin mononucleotide), but, e.g., in fungal LOV proteins, also FAD (Flavin Adenine Dinucleotide). The LOV core is flanked N-and C-terminally by extensions with, in most proteins, α-helical structure (A'α and Jα respectively); these extra secondary structure elements are quite variable as for their length, orientation with respect to the LOV core, and are involved, with diverse mechanisms, in oligomerization and propagation of the light-generated signal.[2–5] LOV domains can exist as standalone proteins (short-LOV) or are associated with a variety of effectors/regulative modules,[6] a feature widely exploited for optogenetic applications.[7,8]

The photophysics and photochemistry of LOV domains relies on the flavin isoalloxazine ring. In the dark adapted state, LOV_{450} (subscripts refer to the approximate absorption maxima), FMN in its fully oxidised state (*ox*) is non-covalently embedded into the protein cavity. BL absorption results in the formation of a photoproduct (LOV_{390}) in which a covalent bond is formed between C4a of FMN and a nearby cysteine. Simultaneously, N5 becomes protonated and the bright green fluorescence of LOV_{450} vanishes (Fig. S1). LOV_{390} is formed via the short-μs decay of the flavin triplet excited state, possibly through the formation of the neutral radical FMNH• (*sq*, neutral semiquinone), although the experimental evidence in favour of the latter reaction is still unclear.[9] In the dark, LOV_{390} returns to the parent state within seconds, minutes, hours or

[a] Institute for Analytical Chemistry, University of Leipzig, Linnéstrasse 3, 04103 Leipzig, Germany
[b] Present address: Max Planck Institute for Biophysical Chemistry, Am Fassberg 11, 37077 Göttingen, Germany
[c] Department of Mathematical, Physical and Computer Sciences, University of Parma, Parco Area delle Scienze 7/A, 43124 Parma, Italy. *: corresponding authir, aba.losi@unipr.it

Electronic Supplementary Information (ESI) available: [details of any supplementary information available should be included here]. See

even days, depending on the specific system.[2] LOV_{390} is held as the signaling state of LOV-photoreceptors, however, LOV domains void of the reactive cysteine can still elicit a functional response, although with lower efficiency, due to conformational changes triggered by the photoreduction with formation of the neutral radical FMNH• and protonation at N5.[10] The efficiency of photoreduction strongly depends on the specific system under investigation considering, e.g., the variant VVD-C108A (VVD is a LOV protein from *Neurospora crassa*), in this protein the neutral radical FMNH• can accumulate also in the presence of oxygen[10] while in other LOV proteins this is possible under anaerobic and reducing conditions.[11] Such observations prompt the investigation of photoreduction in LOV proteins in order to explore the various mechanisms that are possible in flavin-binding photosensitive proteins, both for exploiting them during applications and for understanding of reaction details of native LOV proteins. Recently, the occurrence of the photo-CIDNP (photochemically induced dynamic nuclear polarization, for a recent review see ref [12]) demonstrated that the aromatic amino acid tryptophan can function as internal electron donor towards the photoexcited flavin chromophore.[13] The same work also suggests that tyrosines also can act as electron donors. Phenylalanines, instead, seem not to be able to act as electron donor (see below). A detailed investigation was carried out with iLOV, a Flavin-binding fluorescent protein (FbFp) derived from the LOV2 domain of *Arabidopsis thaliana* phototropin 2 by changing the reactive cysteine into alanine (C426A).[14] iLOV can undergo BL-driven photoreduction of FMN only in the presence of reducing agents, but in the mutated protein Q489D the formation of FMNH• occurs even under aerobic conditions, underscoring the relevance of a proton donor in the vicinity if the chromophore. Transient UV/Vis spectroscopy and electron paramagnetic resonance[15] (EPR) revealed that in iLOV-Q489D a radical pair consisting of the radical anion $FMN^{\bullet -}$ and a radical cation in the protein is formed from the excited triplet state of FMN (^{3}FMN). Further performed mutagenesis of aromatic amino-acids in this protein identified W467 as the main partner, i.e., the strongest quencher for ^{3}FMN via electron transfer, although localised at an edge-to-edge distance of ca. 11 Å (Fig. 1).

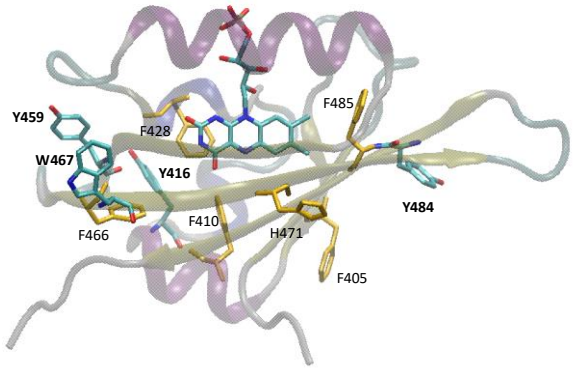

Figure 1. Aromatic amino acids at an edge-to-edge distance <11 Å from the isoalloxazine ring of the FMN chromophore in a LOV domain. Depicted is the structure of iLOV (PDB code 4ees). The closest residues are F485 (5.5 Å) and F410 (5.8 Å), the farthest F405 (10.9 Å) and W467 (10.8 Å). Y416 is localised at 9.9 Å, Y459 at 9.1 Å and Y484 at 10.2 Å. In yellow, positions that have not yet been investigated for their role in photoreduction of FMN (F405, F410, F428, F466, H471, F485).

If this principal electron donor (W467 or W81 using numbering for the LOV core) is replaced with an inert phenylalanine residue, one or more tyrosines in vicinity to the chromophore can take over the role of electron donors, but with lower efficiency. The role of W467 of iLOV as major triplet quencher has been highlighted for applications of LOV domains as genetically encoded photosensitisers for singlet oxygen (SO), in that its substitution in miniSOG (mini Singlet Oxygen Generator, derived from iLOV) enhances the SO quantum yield (Φ_Δ) from 0.03 to 0.61.[16] Accordingly, LOV domains naturally lacking a Trp residue in this position become efficient photosensitisers for SO once the sole reactive cysteine is removed: prominent examples are *Ds*FbFP (engineered from *Dinoroseobacter shibae*) with Φ_Δ = 0.33,[17] and *Mr*4511-C71S or C71G (engineered from *Methylobacterium radiotolerans*) with Φ_Δ = ca. 0.2.[18] Given that formation of SO is a diffusion limited process that implies energy transfer from the triplet excited state of a photosensitiser to O_2, the triplet lifetime (τ_T) is a crucial factor in determining the magnitude of Φ_Δ.[19]

Considering the generic 3D-structure of LOV domains (based on all LOV domain structures published so far) and localizing aromatic amino acids (Fig. 1), it is striking that neither Trp nor Tyr residues are located in close vicinity of the flavin chromophore in LOV domains, i.e., at an edge-to-edge distance <6 Å. Instead, a bunch of redox-inert phenylalanines are amongst the most conserved residues in these photosensing units, in particular F410 and F428 (iLOV numbering), with their aromatic side chains apparently acting as stabilizing factors for the Flavin hetero-aromatic chromophore. In fact, a change of the equivalent position into Tyr in *Cr*-phot-LOV1 (F41Y, LOV1 domain of phototropin from *Chlamydomonas reinhardtii*) impedes formation of the photoproduct, favoring photoreduction of FMN, even if the reactive cysteine is present.[20] It is thus reasonable to suggest that the absence of either Tyr or Trp in close vicinity of the chromophore serves to maximise the yield of the Flavin-cysteine adduct in LOV-based photoreceptors. In this context it is worth mentioning a recent work that analyzed photoreduction starting from a modified version of the fungal LOV protein VVD in which all nine Tyr residues were changed into Phe and also removing the reactive Cys108.[21] Upon introducing step-by-step point mutations in this Tyr-less variant, this research highlighted the relevance of methionines in promoting protonation of the chromophore during photoreduction, and chiefly Met95 was identified as instrumental which is semi-conserved in the LOV series.

The formation of radical pairs between Trp residues and FMN was confirmed by photo-CIDNP in the liquid as well as in the solid state [22]detected by NMR spectroscopy in several LOV proteins void of the reactive cysteine, e.g., in AsPHOT1-LOV2-C450A and Crphot-LOV1-C57S.[23,24] Most recently, *Mr*4511-C71S variants were analysed by this technique;[13] the photo-CIDNP effect was readily detected with the C71S/Q112W variant (Q112 corresponds to W467 in iLOV, edge-to-edge distance ca. 11 Å) (Figs. 1, 2a) and variants with Trp in other positions, Y116W (9 Å), Y129W (11 Å). In contrast, F130W (6 Å) suppressed the CIDNP effect. A new photo-CIDNP effect arises from variant K57W (17 Å) sharing a similar effect with C71S that does not contain any Trp. This finding also indicated that a new electron donor may replace tryptophan and be involved in the photo-

reactions, probably one or more tyrosines, if the tryptophan is absent or relatively far away from FMN.[13]

In this work we further explore *Mr*4511-C71S variants by means of several spectroscopic techniques in order to determine the efficiency by which aromatic amino acids-naturally present or changed at different distances from FMN-are able to quench the excited singlet and triplet states of the chromophore. Furthermore, we determined the values of Φ_Δ with a fluorescent probe. The most notable results are the complete quenching of both singlet and triplet excited state of FMN in C71S/F130W (the closest position to the chromophore analysed), the sequential efficiency of Trp > Tyr > His at position 116 in quenching the triplet state lifetime and the high value of Φ_Δ= 0.44 for C71S/Y116F, simply by introducing a single mutation into the Cys-depleted protein.

Results and discussion

Dynamics of singlet and triplet excited states

In order to estimate the edge-to-edge distances between the FMN chromophore and the here mutated residues we built a homology model of the *Mr*4511 LOV-core (Fig 2a), as previously reported.[13]

The transient triplet-to-triplet absorbance, monitored at 720 nm, decays with a mono-exponential function in all variants investigated, but the value of τ_T is strongly affected by inserting mutations at some of the indicated sites (Fig 2b-d, Table 1).

Position 116 is paradigmatic: in *Mr*4511 it is naturally occupied by a Tyr residue and the decay of the triplet is slowed down by inserting a Phe residue or, to a lesser extent, a histidine; on the contrary, the decay is strongly accelerated by a Trp residue. This observation is in agreement with the efficiency of aromatic amino-acids in quenching the triplet state of free ^{3}FMN via electron transfer reactions, i.e. Trp> Tyr>His.[25] This reflects the standard reduction potentials of these amino-acids: $E^0_{Trp+./Trp} \approx +0.85$ V, $E^0_{Tyr+./Tyr} \approx +1.1$ V, $E^0_{His+./His} \approx +1.3$ V.[26] Trp appears as a strong quencher for ^{3}FMN for all positions tested with the exception of K57W for which the edge-to-edge distance is larger than 15 Å (Fig. 2a, c). At distances less than 10 Å, instead, Trp can also quench the singlet excited state as demonstrated by the lower values for fluorescence quantum yields (Φ_F) and lifetimes (τ_F) in the variants C71S/Y116W, C71S/Y129W, and, most notably, in C71S/F130W, for which Φ_F becomes negligible and τ_F is shorter than the resolution limit of our setup (Table 1 and Figure S2). This residue is at an edge-to-edge distance of ~ 6 Å from FMN: a Trp in this position impairs fluorescence and intersystem crossing to form ^{3}FMN formation (Fig. 2c), even though if such residue is inserted into the WT Mr4511 protein (F130W), i.e., when the reactive cysteine is present (Figs. 2e and S2). Under our conditions (aerobic aqueous solutions, no reducing agent present), no FMN radicals could be accumulated when the samples were continuously illuminated with BL (Fig. S3).

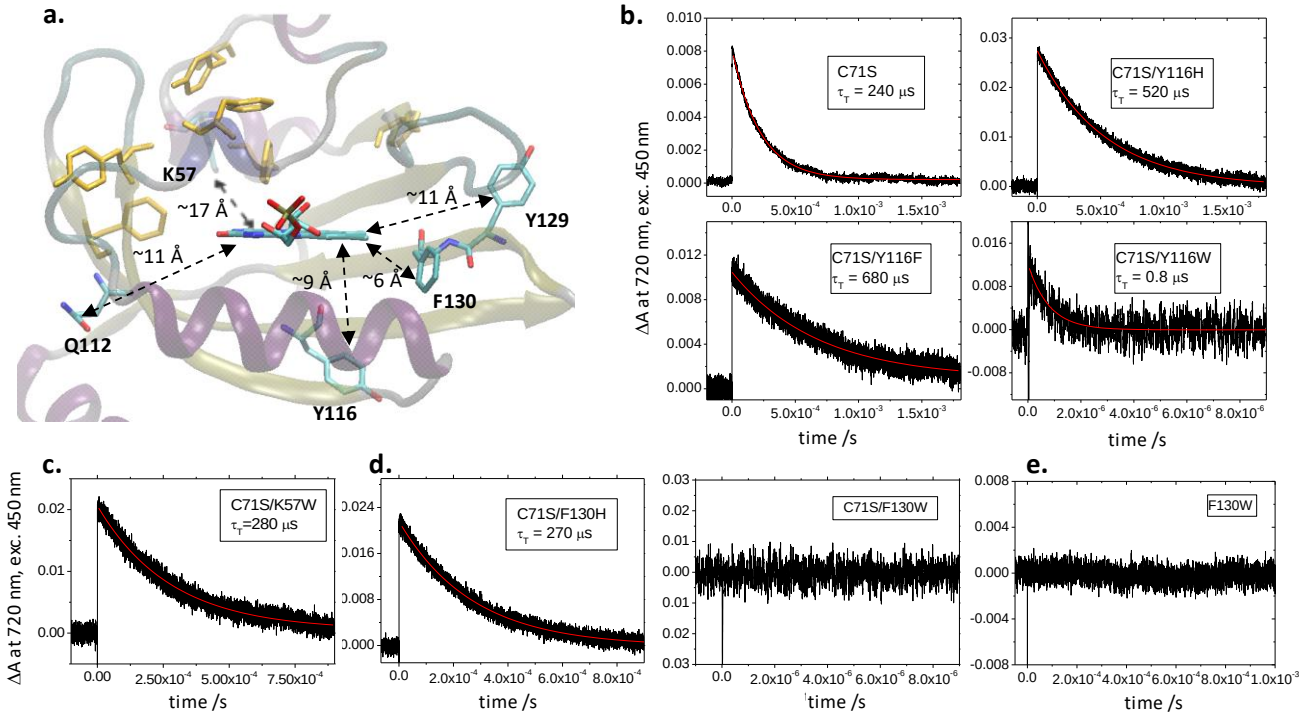

Figure 2. **a.** Homology model of *Mr*4511 with evidenced mutated residues and edge-to-edge distances from the FMN chromophore; the ribityl chain of FMN with the terminal phosphate group points towards the viewer (see Figure S2 for another orientation); **b.** Triplet state quenching effects from aromatic amino-acids at position 116, occupied by a Tyr in the native protein and in the C71S variant; the most effective quencher is Trp, the less efficient one is Phe; **c.** A Trp inserted at position 57, ca. 17 Å away from FMN, does not quench the triplet state; **d.** Insertion of a His residue at position 130 (d1) has an only negligible effect on the triplet lifetime (τ_T), whereas, however, insertion of a Trp residue at this position (d2) impedes formation of the triplet state, even if (**e.**) the reactive Cys71 is present.

Table 1. Triplet lifetimes (τ_T), fluorescence quantum yields (Φ_F) and fluorescence lifetimes (τ_F)

Molecule	[a]τ_T/μs	[a]Φ_F	[a]τ_F/ns
FMN	3.5	0.25	4.2
***Mr*4511 variants**			
C71S[b]	240	0.35	4.0
C71S/Q112W[b]	24.7	0.32	3.8
C71S/K57W	280	0.33	3.9
C71S/Y116F	690	0.36	4.0
C71S/Y116H	520	0.36	4.0
C71S/Y116W	0.83	0.17	<2.0>[d]
C71S/Y129H	300	0.34	3.9
C71S/Y129W	30	0.28	3.4
C71S/F130H	270	0.31	3.7
C71S/F130W	N.D.	1.5×10^{-3}	< 0.1
WT[c]	2.0	0.14	1.9
F130W	N.D.	2.1×10^{-3}	< 0.1

[a]: errors are within 10%; [b]:[18]; [c]:[27]; [d]:τ_1 =1.0 ns (21%), τ_1 =2.3 ns (79%)

Triplet formation and singlet oxygen quantum yields

Pulsed photoacoustics (PA) allows to determine the quantum yield of formation of triplet states without the need to employ standard compounds as actinometers, i.e., this method works in absolute terms, solely based on energy balance considerations (eq. 4a in Experimental).[28] The PA signals are in general composed of two contributions, one arising from thermal decays (α_i) and the other generated from volume changes of non-thermal origin (ΔV_i), e.g., protein conformational changes or rearrangement of weak interactions.[29] It is thus mandatory to separate both contributions in the PA signal; basically this can be done by performing measurements at different temperatures, making advantage of the fact that the value of β, the volume expansion coefficient, strongly depends on temperature in aqueous solutions (see Experimental for details): at a given temperature, $T_{\beta=0}$, the thermal contribution vanishes and the PA signal recorded from a sample is solely due to ΔV_i. The striking difference between certain variants investigated here is demonstrated in Fig. 3..

C71S/K57W has similar features as C71S (Table 2) with a small photoacoustic (PA) signal at $T_{\beta>0}$, due to the high fluorescence efficiency (therefore resulting relatively low efficiency of non-radiative decays) and the negative ΔV, immediately visible at $T_{\beta=0}$. On the contrary, for C71S/F130W non-radiative decays occur on the ns time-scale with nearly 100% efficiency, no light induced ΔV are detected, and basically this variant behaves like a photocalorimetric reference compound that releases all the excitation energy as heat within few ps.[30] The PA data are thus fully in line with the UV/Vis data reported above.

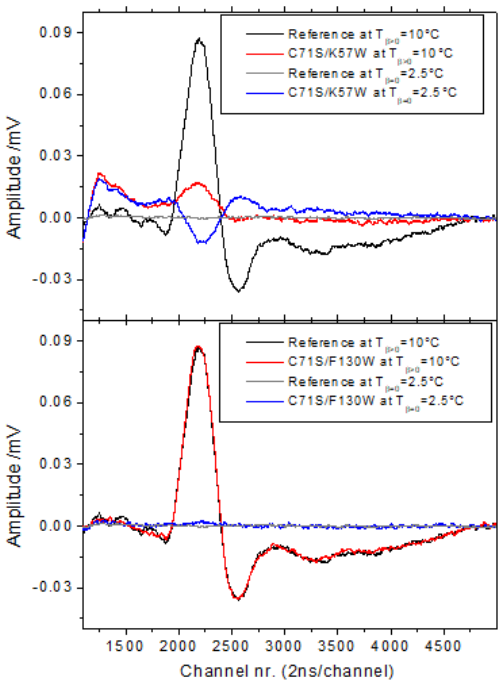

Figure 3. PA signals at $T_{\beta=0}$ = 2.5 °C and at $T_{\beta>0}$ = 10 °C for top, C71S/K57W and, bottom, C71S/F130W. At $T_{\beta=0}$ the signal for the reference compound (new coccine) is a zero line. The variant C71S/F130W behaves very similar to new coccine.

Table 2 Triplet quantum yields (Φ_T), molecular volume changes (ΔV_T), and quantum yields of singlet oxygen formation (Φ_Δ)

Molecule	[a]Φ_T	[a]ΔV_T ml/mol	[a]Φ_Δ
FMN	0.55	-3.3	0.56[31]
***Mr*4511 variants**			
C71S	0.50	-2.0	0.17
C71S/Q112W	0.56	-1.6	< 0.01
C71S/K57W	0.55	-1.7	0.13
C71S/Y116F	0.61	-2.2	0.44
C71S/Y116H	0.61	-2.0	0.21
C71S/Y116W	0.44	-2.6	0.02
C71S/Y129H	0.56	-2.9	0.22
C71S/Y129W	0.58	-2.0	0.08
C71S/F130H	0.71	-1.5	0.17
C71S/F130W	<0.05	N.A.	< 0.01
F130W	<0.05	N.A.	0.02

[a]: errors are within 10%

For each variant and for free FMN, triplet formation produces a negative volume change ($\Delta V_T < 0$), most probably due to the rearrangement of weak interactions following charge redistribution (Table 2).[29]

The sole protein for which the value of τ_T falls within the time window of PA is C71S/Y116W (Table 1). Time resolution was readily achieved at each temperature and the kinetics follows a sharp Arrhenius behaviour (Fig. S4). The absorbed energy is fully dissipated, also considering the lack of fluorescence, indicating that no long-lived species is formed. The negative ΔV_T is also fully compensated by an expansion concomitant with the triplet decay (Table S2)

Finally, we evaluated the photosensitized formation of singlet oxygen (Φ_Δ) by using the fluorescent probe Singlet Oxygen Sensor Green (SOSG), in a comparative set-up as previously reported.[18] As expected, mutations inducing fast triplet decay or preventing triplet formation resulted in very low values of Φ_Δ (Table 2). The variant C71S/Y116F shows instead a quite high Φ_Δ= 0.44 (Fig. 4, top), with only two mutations with respect to the WT Mr4511 protein, making it one of the most efficient genetically encoded photosensitizers.[32] Not surprisingly, as energy transfer to O_2 from the excited triplet state is a diffusion limited process,[33] the value of Φ_Δ increases with τ_T (Fig. 4, bottom), although other factors might be involved (e.g., structural modifications induced by the mutations that influence ingress of O_2 and egress of singlet oxygen). Although it is known that LOV domains engineered as photosensitisers are prone to form also other reactive oxygen species (ROS) besides SO, [17]we have previously shown that SOSG provides for the C71S and C71G values of Φ_Δ comparable to those obtained with SO direct detection by phosphorescence.[18] Even if we cannot exclude formation of ROS such as H_2O_2, we thus suggest that SO is the most relevant species formed with the variants of *Mr*4511 studied here. Another important aspect for applications is photobleaching during prolonged illumination, a relevant phenomenon in miniSOG and related proteins.[34]Under the experimental conditions used in this work we did not observe photobleaching, but we cannot exclude that such a degradation of the protein may occur in cells or tissues: only experiments *in vivo* will be able to clarify this point and assess the potential of Mr4511 variants as robust photosensitisers for applications.

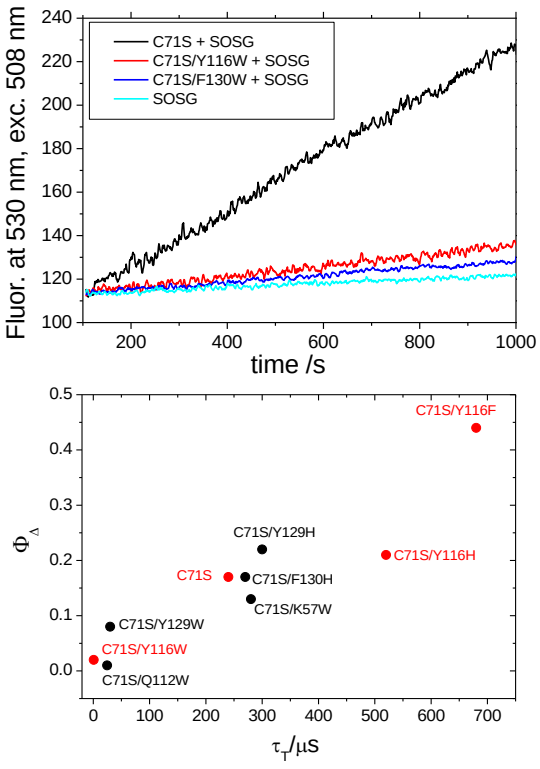

Figure 4. Top, kinetics of the photosensitized formation of singlet oxygen as monitored from the increase in fluorescence of SOSG (see experimental) in the presence of BL and of Mr4511 variants. SOSG alone is also included as control; bottom, singlet oxygen quantum yield plotted as a function of the triplet lifetime. Red symbols highlight the Y116X series.

Experimental

Samples preparations and handling

All genetic manipulations followed standard protocols. Cloning of *Mrad2831_4511* from genomic DNA, expression of the wildtype (WT) *Mr*4511 LOV-protein, and generation of the C71S mutated protein is described elsewhere.[18,27] Variants C71SK57W, C71SY116F/H/W, C71SY129H/W, and C71SF130H/W were PCR-generated using primers P1-P16 (Table S1) and using the formerly generated C71S protein as template. Mutation F130W was generated with the same primers P15 and P16, except for using the WT-encoding plasmid as template. The ligation products were transformed into *Escherichia coli* BL21 (DE3) cells. All *Mr*4511 protein variants had been furnished with a C-terminal His_6 tag. Proteins were expressed by the following protocol: the transformed cells were cultured in DYT medium (16 g Trypton, 10 g yeast-extract, 5 g NaCl in 1 L distilled water), supplemented with kanamycin (20 µg mL^{-1}). After induction with isopropyl β-D-thiogalactoside, IPTG, (1 mM final concentration) for 16 hours at 16 °C, cells were harvested by centrifugation at 6500 rpm (Beckman Coulter, Avanti™ J-20 XP, JA-10) for 5 min at 4 °C and washed with distilled water. For protein purification, the cell pellets were resuspended in ice-cold KPB buffer (20 mM, pH 8.0) containing 0.3 M NaCl, and the cells were disrupted by an ultrasonifier (0 °C, pulse on: 1 s, pulse off: 2 s, total duration time of 24 min; Nanjing Safer Biotech). The suspension was centrifuged at 15000 rpm (Beckman Coulter, Optima™ L-80 XP Ultracentrifuge, Ti-60) for 60 min at 4 °C. The supernatants were collected and purified via Ni^{2+}-affinity chromatography on chelating sepharose (GE healthcare). After elution from the Ni^{2+}-affinity column, imidazole was removed by dialysis against Na-phosphate buffer (10 mM, pH 8.0, 100 mM NaCl) containing NaCl (100 mM) or in K-phosphate buffer (50 mM, pH 8.0, 300 mM NaCl), as detailed in the supplementary information (Fig. S2). Structural modeling was with SWISS-MODEL in the automated mode,[35] graphical rendering with VMD (Figs. 1, 2a, S1).[36]

UV/Vis spectroscopy

Steady state absorption an fluorescence spectra were recorded at (20 ± 1) °C with a Jasco 7850 UV/Vis spectrophotometer (Jasco

Europe, Cremella, LC, Italy) and a Perkin-Elmer LS50 luminescence spectrometer (PerkinElmer, Waltham, MA, USA), respectively. Fluorescence quartz cuvettes (10×4) mm with 10 mm path length were used. The fluorescence quantum yields (Φ_F) were measured as relative values,[37] using FMN as reference (Φ_F = 0.26[38]). Fluorescence lifetimes (τ_F) were measured using the FLS920 instrumentation (Edinburgh Instruments, Livingston, UK) based on the Time-Correlated Single-Photon Counting (TCSPC) protocol.[39] The sample excitation was achieved through a pulsed LED with maximum emission at 450 nm, 6 MHz repetition rate (PicoQuant, Berlin, Germany). The sample absorbance at the excitation wavelength was kept at ca. 0.08. The Instrument Response Function (IRF) was determined at the excitation wavelength using a very diluted solution of colloidal silica (LUDOX). In order to ensure that only one photon per light pulse was detected, the photon rate did not exceed 5% of the exciting-light rate.[8] Data were analysed using the F900 Software (Edinburgh instruments, Livingston, UK); in case the fluorescence decay was found not mono-exponential, the average fluorescence lifetime $\langle\tau_F\rangle$ was calculated according to eq.1:

$$\langle\tau_F\rangle = \sum \tau_i f_i \qquad \text{eq. 1}$$

where τ_i is the lifetime of the *i*-th-component and f_i the associated fraction of the total amplitude.

Time-resolved flash photolysis was employed to measure the triplet lifetime (decay of the triplet-to-triplet absorbance) in the µs-to-ms time range, as described.[27] Samples were excited by a laser pulse (duration about 10 ns, energy always kept below 1.5 mJ per pulse), obtained from an OPO (GWU Lasertechnik- Erftstadt, Germany, built into the InnoLas cage), which was driven by the third harmonic (355 nm) of a Q-switched Nd:YAG laser (InnoLas, Krailling, Germany).[37] Kinetics were monitored by means of a further optical line: two monochromators (master and slave) selected the probe wavelength from a continuous-wave 75 W Xenon lamp (AMKO, Utting, Germany). Triplet-triplet absorption decay for *Mr*4511 proteins was monitored at 720 nm, after single shot excitation at 450 nm.

Determination of the singlet oxygen quantum yields (Φ_Δ) was performed by using the fluorescence probe Singlet Oxygen Sensor Green (SOSG, Thermo Fisher Scientific, Waltham, MA-USA). The content of one vial of SOSG was dissolved in 33 µl of methanol to serve as stock solution of ≈ 5 mM. From this, a working solution of ≈ 10 µM was prepared in buffer immediately before use. Concentrations used for measurements were ≈ 2 µM of SOSG and ≈ 8 µM of protein/FMN in Na-Pi buffer (10 mM, 100 mM NaCl, pH=8). The increase in SOSG fluorescence was monitored at 530 nm exciting the sample at 508 nm (to minimize FMN absorbance) and keeping the cuvette illuminated from above with an LED (maximum emission = 455 nm, LED455, Roithner LaserTechnik, Wien, Austria), operating at ca. 3 mW.[37] Control measurements were performed with: i) SOSG alone with matched concentration as in the sample containing SOSG and the photosensitizer (protein or FMN); ii) protein/FMN alone with matched concentration as in the sample containing SOSG and the photosensitizer, as described previously.[18]

Pulsed photoacoustics

Time-resolved photoacoustic (PA) measurements were performed to determine triplet quantum yields (Φ_T) and structural volume changes of non-thermal origin (ΔV).Excitation at 450 nm was achieved with the same ns laser employed for transient UV-Vis spectroscopy.[28] The samples (ca. 2.8 mL) were temperature controlled to ± 0.02 °C in the cuvette holder FLASH 100 (Quantum Northwest, Spokane, WA, USA). PA signals were detected by a V103-RM ultrasonic transducer and fed into a 5662 preamplifier (Panametrics Inc., Waltham, MA, USA). The laser beam was shaped by a 1 × 12 mm slit. The pulse energy was measured with a pyroelectric energy meter (RJP735 head connected to a meter RJ7620 from Laser Precision Corp). The experiments were performed in the linear regime of amplitude versus laser fluence. The dye new coccine (FLUKA, Neu-Ulm, Germany) was used as a calorimetric reference.[30] Deconvolution of PA signals was performed with the software Sound Analysis 3000 (Quantum Northwest Inc., Spokane, WA) assuming that the time evolution of the pressure is composed of a sum of exponential functions. The analysis yields the fractional amplitudes (φ_i) and the lifetimes (τ_i) of the transients, in a time window between 20 ns and 10 µs and a time resolution of ca. 60 ns. [40] At a given temperature and for each resolved *i*-th step, the fractional (with respect to the reference compound, see caption of Fig. S4) amplitude φ_i is the sum of the fraction of absorbed energy released as heat (α_i) and the structural volume change *per* absorbed Einstein (ΔV_i), according to eq.3:[41]

$$\varphi_i = \alpha_i + \frac{\Delta V_i}{E_\lambda}\frac{c_P\rho}{\beta} \qquad \text{eq. 3}$$

where E_λ is the molar excitation energy, $\beta = (\partial V/\partial T)_p \Delta V$ is the volume expansion coefficient, c_p is the heat capacity at constant pressure, and ρ is the mass density of the solvent. At each temperature, four deconvolution results were accumulated. The "two temperature" (TT) method was used in order to separate α_i from ΔV_i.[28] The sample waveform was acquired at a temperature for which heat transport is zero, $T_{\beta=0}$ = 2.5 °C and -1.3°C for the buffers employed here (respectively NaPi 10 mM, pH 8.0, 100 mM NaCl); KPi 50 mM, pH 8.0, 300 mM NaCl), and at a higher temperature, $T_{\beta>0}$ = 10 °C. The thermoelastic parameters of the solvent are determined by comparison with those of ditilled water, that are tabulated. At $T_{\beta=0}$ the PA signal is only due to ΔV_i, while at 10 °C both heat release and ΔV_i contribute to the sample signal. The reference for deconvolution was recorded at $T_{\beta>0}$ and data were handled as previously reported.[28] In some instances, detailed in the text, we also applied the several temperature (ST) method, for which PA signals were recorded and deconvoluted between 3 and 20°C: both α_i and ΔV_i can be determined from the linear plots of φ_i vs. $c_p\rho/\beta$.[29]

For photochemically active LOV proteins, for which the triplet state decays within few µs into the photoproduct, PA signals are best fitted by a two exponential function.[27,28] The unresolved, "prompt" step (τ_1 < 20 ns) is assigned to formation of the FMN triplet state (subscript T). The µs process corresponds to formation of the photoproduct (subscript P). Deconvolution directly provides the products $\Phi_T E_T$ and $\Phi_P E_P$ (Eqn. 4a and 4b), referring to the quantum

yield of formation for the triplet state and adduct, respectively, multiplied by the energy level of the two transients[42]:

$$\Phi_{\mathrm{T}}\frac{E_{\mathrm{T}}}{E_{\lambda}} = 1 - \alpha_1 - \Phi_{\mathrm{F}}\frac{E_{\mathrm{F}}}{E_{\lambda}} \qquad \text{eq. 4a}$$

$$\alpha_2 = \Phi_{\mathrm{T}}\frac{E_{\mathrm{T}}}{E_{\lambda}} - \Phi_{\mathrm{P}}\frac{E_{\mathrm{P}}}{E_{\lambda}} \qquad \text{eq. 4b}$$

where E_F is the average energy for the fluorescence emission (232 kJ/mol for LOV proteins), and E_λ= 265.84 kJ/mol is the photonic excitation energy (λ_{ex} = 450 nm). E_T = ca. 200 kJ/mol for LOV proteins as in the case of free FMN.[43–46] With few exceptions, as detailed in the text, the triplet decay of C71S variants falls outside the PA window. The molecular volume changes that the *Mr*4511 proteins experience upon formation of the flavin triplet state (ΔV_T) (with respect to the unphotolyzed state) can be calculated from eqn. (5)

$$\Delta V_{\mathrm{T}} = \frac{\Delta V_1}{\Phi_{\mathrm{T}}} \qquad \text{eq. 5}$$

Conclusions

The data illustrated in this work evidenced that Trp and Tyr in the vicinity of the chromophore can intefere with ^{3}FMN decay kinetics, as well as with triplet state formation already at a distance of ca. 9Å (C71S/Y116W) and most dramatically at 6 Å (C71S/F130W), by quenching the FMN singlet excited state. This latter process is so efficient with Trp residues, that in Mr4511-F130W formation of the photoproduct is hindered, even if the reactive cysteine is present. In the aerobic, non reducing solutions used here, the radical pairs as detected with CIDNP[13] do not accumulate, apparently recombination is very fast as suggested by the PA results with C71S/Y116W. Phe residues appears quite innocent and can be positioned at suitable distances from FMN to increase the yield of singlet oxygen formation, contributing to the rational design of LOV-based photosensitisers.

Conflicts of interest

There are no conflicts to declare

Notes and references

1 J. T. Henry and S. Crosson, Ligand-Binding PAS Domains in a Genomic, Cellular, and Structural Context, *Annu. Rev. Microbiol.*, 2011, **65**, 261–286.

2 A. Losi and W. Gärtner, Solving Blue Light Riddles: New Lessons from Flavin-binding LOV Photoreceptors, *Photochem. Photobiol.*, 2017, **93**, 141–158.

3 J. P. Zayner, T. Mathes, T. R. Sosnick and J. T. M. Kennis, Helical Contributions Mediate Light-Activated Conformational Change in the LOV2 Domain of Avena sativa Phototropin 1, *ACS Omega*, 2019, **4**, 1238–1243.

4 J. N. Iuliano, J. T. Collado, A. A. Gil, P. T. Ravindran, A. Lukacs, S. Shin, H. A. Woroniecka, K. Adamczyk, J. M. Aramini, U. R. Edupuganti, C. R. Hall, G. M. Greetham, I. V. Sazanovich, I. P. Clark, T. Daryaee, J. E. Toettcher, J. B. French, K. H. Gardner, C. L. Simmerling, S. R. Meech and P. J. Tonge, Unraveling the Mechanism of a LOV Domain Optogenetic Sensor: A Glutamine Lever Induces Unfolding of the Jα Helix, *ACS Chem. Biol.*, 2020, **15**, 2752–2765.

5 K. Magerl and B. Dick, Dimerization of LOV domains of: Rhodobacter sphaeroides (RsLOV) studied with FRET and stopped-flow experiments, *Photochem. Photobiol. Sci.*, 2020, **19**, 159–170.

6 S. T. Glantz, E. J. Carpenter, M. Melkonian, K. H. Gardner, E. S. Boyden, G. K.-S. Wong and B. Y. Chow, Functional and topological diversity of LOV domain photoreceptors, *Proc. Natl. Acad. Sci. U. S. A.*, 2016, **113**, E1442-1451.

7 A. Losi, K. H. Gardner and A. Möglich, Blue-Light Receptors for Optogenetics, *Chem. Rev.*, 2018, **118**, 10659–10709.

8 E. E. Berlew, I. A. Kuznetsov, K. Yamada, L. J. Bugaj and B. Y. Chow, Optogenetic Rac1 engineered from membrane lipid-binding RGS-LOV for inducible lamellipodia formation, *Photochem. Photobiol. Sci.*, 2020, **19**, 353–361.

9 C. Bauer, C.-R. Rabl, J. Heberle and T. Kottke, Indication for a Radical Intermediate Preceding the Signaling State in the LOV Domain Photocycle, *Photochem. Photobiol.*, 2011, **87**, 548–553.

10 E. F. Yee, R. P. Diensthuber, A. T. Vaidya, P. P. Borbat, C. Engelhard, J. H. Freed, R. Bittl, A. Möglich and B. R. Crane, Signal transduction in light-oxygen-voltage receptors lacking the adduct-forming cysteine residue, *Nat. Commun.*, 2015, **6**, 1–10.

11 K. Lanzl, M. V. Sanden-Flohe, R. J. Kutta and B. Dick, Photoreaction of mutated LOV photoreceptor domains from Chlamydomonas reinhardtii with aliphatic mercaptans: Implications for the mechanism of wild type LOV, *Phys. Chem. Chem. Phys.*, 2010, **12**, 6594–6604.

12 J. Matysik, Y. Ding, Y. Kim, P. Kurle, A. Yurkovskaya, K. Ivanov and A. Alia, Photo-CIDNP in Solid State, *Appl. Magn. Reson.*, 2021, *in press*, DOI:10.1007/s00723-021-01322-5.

13 Y. Ding, A. S. Kiryutin, Z. Zhao, Q. Z. Xu, K. H. Zhao, P. Kurle, S. Bannister, T. Kottke, R. Z. Sagdeev, K. L. Ivanov, A. V. Yurkovskaya and J. Matysik, Tailored flavoproteins acting as light-driven spin machines pump nuclear hyperpolarization, *Sci. Rep.*, 2020, **10**, 18658.

14 M. Wingen, J. Potzkei, S. Endres, G. Casini, C. Rupprecht, C. Fahlke, U. Krauss, K.-E. Jaeger, T. Drepper and T. Gensch, The photophysics of LOV-based fluorescent proteins--new tools for cell biology., *Photochem. Photobiol. Sci.*, 2014, **13**, 875–83.

15 B. Kopka, K. Magerl, A. Savitsky, M. D. Davari, K. Röllen, M. Bocola, B. Dick, U. Schwaneberg, K.-E. Jaeger and U. Krauss, Electron transfer pathways in a light, oxygen, voltage (LOV) protein devoid of the photoactive cysteine, *Sci. Rep.*, 2017, **7**, 13346.

16 M. Westberg, M. Bregnhøj, M. Etzerodt and P. R. Ogilby, No Photon Wasted: An Efficient and Selective Singlet Oxygen Photosensitizing Protein, *J. Phys. Chem. B*, 2017, **121**, 9366–9371.

17 S. Endres, M. Wingen, J. Torra, R. Ruiz-González, T. Polen, G. Bosio, N. L. Bitzenhofer, F. Hilgers, T. Gensch, S. Nonell, K.-E. Jaeger and T. Drepper, An optogenetic toolbox of LOV-based photosensitizers for light-driven killing of bacteria., *Sci. Rep.*, 2018, **8**, 15021.

18 E. Consiglieri, Q. Xu, M. Bregnhøj, M. Westberg, P. R. Ogilby and A. Losi, Single mutation in a novel bacterial LOV protein yields a singlet oxygen generator, *Photochem. Photobiol. Sci.*, 2019, **18**, 2657–2660.

19 P. R. Ogilby, Singlet oxygen: there is indeed something new under the sun, *Chem. Soc. Rev.*, 2010, **39**, 3181.

20 K. Magerl, I. Stambolic and B. Dick, Switching from adduct formation to electron transfer in a light–oxygen–voltage domain containing the reactive cysteine, *Phys. Chem. Chem. Phys.*, 2017, **19**, 10808–10819.

21 E. F. Yee, S. Oldemeyer, E. Böhm, A. Ganguly, D. M. York, T. Kottke and B. R. Crane, Peripheral Methionine Residues Impact Flavin Photoreduction and Protonation in an Engineered LOV Domain Light Sensor, *Biochemistry*, 2021, **12**, doi.org/10.1021/acs.biochem.1c00064.

22 G. Richter, S. Weber, W. Römisch, A. Bacher, M. Fischer and W. Eisenreich, Photochemically Induced Dynamic Nuclear Polarization in a C450A Mutant of the LOV2 Domain of the Avena s ativa Blue-Light Receptor Phototropin, *J. Am. Chem. Soc.*, 2005, **127**, 17245–17252.

23 S. S. Thamarath, J. Heberle, P. J. Hore, T. Kottke and J. Matysik, Solid-state photo-CIDNP effect observed in phototropin LOV1-C57S by 13C magic-angle spinning NMR spectroscopy, *J. Am. Chem. Soc.*, 2010, **132**, 15542–15543.

24 Y. Ding, A. S. Kiryutin, A. V. Yurkovskaya, D. V. Sosnovsky, R. Z. Sagdeev, S. Bannister, T. Kottke, R. K. Kar, I. Schapiro, K. L. Ivanov and J. Matysik, Nuclear spin-hyperpolarization generated in a flavoprotein under illumination: experimental field-dependence and theoretical level crossing analysis, *Sci. Rep.*, 2019, **9**, 1–11.

25 Y. P. Tsentalovich, J. J. Lopez, P. J. Hore and R. Z. Sagdeev, Mechanisms of reactions of flavin mononucleotide triplet with aromatic amino acids, *Spectrochim. Acta - Part A Mol. Biomol. Spectrosc.*, 2002, **58**, 2043–2050.

26 D. M. Close and P. Wardman, Calculation of Standard Reduction Potentials of Amino Acid Radicals and the Effects of Water and Incorporation into Peptides, *J. Phys. Chem. A*, 2018, **122**, 439–445.

27 E. Consiglieri, Q. Xu, K.-H. Zhao, W. Gärtner and A. Losi, First molecular characterisation of blue- and red-light photoreceptors from *Methylobacterium radiotolerans*, *Phys. Chem. Chem. Phys.*, 2020, **22**, 12434–12446.

28 S. Raffelberg, M. Mansurova, W. Gärtner and A. Losi, Modulation of the photocycle of a LOV domain photoreceptor by the hydrogen-bonding network, *J. Am. Chem. Soc.*, 2011, **133**, 5346–5356.

29 A. Losi and S. E. Braslavsky, The time-resolved thermodynamics of the chromophore–protein interactions in biological photosensors as derived from photothermal measurements, *Phys. Chem. Chem. Phys.*, 2003, **5**, 2739–2750.

30 S. Abbruzzetti, C. Viappiani, D. H. Murgida, R. Erra-Balsells and G. M. Bilmes, Non-toxic, water-soluble photocalorimetric reference compounds for UV and visible excitation, *Chem. Phys. Lett.*, 1999, **304**, 167–172.

31 M. Westberg, M. Bregnhøj, M. Etzerodt and P. R. Ogilby, Temperature Sensitive Singlet Oxygen Photosensitization by LOV-Derived Fluorescent Flavoproteins, *J. Phys. Chem. B*, 2017, **121**, 2561–2574.

32 M. Westberg, L. Holmegaard, F. M. Pimenta, M. Etzerodt and P. R. Ogilby, Rational design of an efficient, genetically encodable, protein-encased singlet oxygen photosensitizer., *J. Am. Chem. Soc.*, 2015, **137**, 1632–42.

33 M. C. DeRosa and R. J. Crutchley, Photosensitized singlet oxygen and its applications, *Coord. Chem. Rev.*, 2002, **233**–**234**, 351–371.

34 J. Torra, C. Lafaye, L. Signor, S. Aumonier, C. Flors, X. Shu, S. Nonell, G. Gotthard and A. Royant, Tailing miniSOG: structural bases of the complex photophysics of a flavin-binding singlet oxygen photosensitizing protein, *Sci. Rep.*, 2019, **9**, 2428.

35 M. Biasini, S. Bienert, A. Waterhouse, K. Arnold, G. Studer, T. Schmidt, F. Kiefer, T. Gallo Cassarino, M. Bertoni, L. Bordoli and T. Schwede, SWISS-MODEL: modelling protein tertiary and quaternary structure using evolutionary information., *Nucleic Acids Res.*, 2014, **42**, W252-8.

36 W. Humphrey, A. Dalke and K. Schulten, VMD: Visual molecular dynamics, *J. Mol. Graph.*, 1996, **14**, 33–38.

37 E. Consiglieri, A. Gutt, W. Gärtner, L. Schubert, C. Viappiani, S. Abbruzzetti and A. Losi, Dynamics and efficiency of photoswitching in biliverdin-binding phytochromes, *Photochem. Photobiol. Sci.*, 2019, **18**, 2484–2496.

38 P. A. . van den Berg, J. Widengren, M. A. Hink, R. Rigler and A. J. W. . Visser, Fluorescence correlation spectroscopy of flavins and flavoenzymes: photochemical and photophysical aspects, *Spectrochim. Acta Part A Mol. Biomol. Spectrosc.*, 2001, **57**, 2135–2144.

39 J. R. Lakowicz, *Principles of Fluorescence Spectroscopy Joseph R . Lakowicz*, 3rd edn., 2006.

40 J. E. Rudzki, J. L. Goodman and K. S. Peters, Simultaneous determination of photoreaction dynamics and energetics using pulsed, time-resolved photoacoustic calorimetry, *J. Am. Chem. Soc.*, 1985, **107**, 7849–7854.

41 S. E. Braslavsky and G. E. Heibel, Time-resolved photothermal and photoacoustic methods applied to photoinduced processes in solution, *Chem. Rev.*, 1992, **92**, 1381–1410.

42 A. Losi and S. E. Braslavsky, The time-resolved thermodynamics of the chromophore-protein interactions in biological photosensors as derived from photothermal measurements, *Phys. Chem. Chem. Phys.*, 2003, **5**, 2739–2750.

43 M. Gauden, S. Crosson, I. H. M. van Stokkum, R. van Grondelle, K. Moffat and J. T. M. Kennis, eds. S. Avrillier and J.-M. Tualle, International Society for Optics and Photonics, 2004, vol. 5463, p. 97.

44 A. Losi, E. Polverini, B. Quest and W. Gärtner, First Evidence for Phototropin-Related Blue-Light Receptors in Prokaryotes, *Biophys. J.*, 2002, **82**, 2627–2634.

45 A. Losi, B. Quest and W. Gärtner, Listening to the blue: The time-resolved thermodynamics of the bacterial blue-light receptor YtvA and its isolated LOV domain, *Photochem. Photobiol. Sci.*, 2003, **2**, 759–766.

46 A. Losi, T. Kottke and P. Hegemann, Recording of blue light-induced energy and volume changes within the wild-type and mutated phot-LOV1 domain from Chlamydomonas reinhardtii., *Biophys. J.*, 2004, **86**, 1051–60.